Journal of Chromatography A, 1217 (2010) 6373–6381

Contents lists available at ScienceDirect

Journal of Chromatography A

journal homepage: www.elsevier.com/locate/chroma

On the optimization of the shell thickness of superficially porous particles

Krisztián Horváth[a,b], Fabrice Gritti[a], Jacob N. Fairchild[a], Georges Guiochon[a,*]

[a] University of Tennessee, Department of Chemistry, Knoxville, TN, 37996-1600, USA
[b] University of Pannonia, Department of Analytical Chemistry, P.O. Box 158, Veszprém, H-8200, Hungary

ARTICLE INFO

Article history:
Received 17 May 2010
Received in revised form 28 July 2010
Accepted 6 August 2010
Available online 19 August 2010

Keywords:
Superficially porous particles
Shell thickness
General rate model
Poppe plot
Extra-column volume

ABSTRACT

The thickness of the porous shells of superficially porous particles influences the separation power of columns packed with these packing materials. Models of the mass transfer kinetics across porous adsorbents permit the prediction of the HETP curves of columns packed with particles having shells of different thicknesses, for molecules of different sizes. Decreasing the thickness of the porous layer potentially results in lower values of the "C-term" of the HETP curve and of the minimum of these curves. The Poppe plots calculated under isocratic and gradient conditions show that the separation power of columns packed with superficially porous particles increases significantly with decreasing thickness of the porous layer but this increase is more important for larger than for smaller molecules. The resolution between pairs of compounds increases at constant values of their retention factors when the strength of the eluent must be reduced to compensate for the decrease of their retention that is caused by the reduction of the surface area of the stationary phase. Thus, the separation power of columns packed with superficially porous particles increases with decreasing shell thickness. In contrast, if analysts do not compensate for the retention decrease, the resolution between small molecular weight compounds becomes worse with thin than with thick superficially porous particles. Finally, the importance of using instruments providing low extra-column band broadening contributions is stressed.

1. Introduction

Modern analytical applications of liquid chromatography require columns with higher and higher efficiencies. The use of monolithic silica rods [1–3], of sub-2 μm particles, or of superficially porous particles [4–7] offers today the most satisfactory results. Due to their excessive radial heterogeneity, the efficiency of monolithic columns currently available is lower than that of columns packed with 3 μm particles, let alone sub-2 μm particles. However, columns packed with fine particles have a low permeability and the achievement of the improved efficiency offered by modern packed columns comes at a high price: it requires the use of very high operating pressures (700–1000 bar). The most advanced chromatographs for VHPLC are able to operate at inlet pressures up to 1200 bar. Changing existing and, usually, well operating chromatographic systems, is most expensive, which is not always an acceptable option. An alternate possibility to overcome the limitations due to the use of sub-2 μm particles and of monolithic silica rods is the use of superficially porous particles [4,6]. Columns packed with these particles proved to be very efficient, providing efficiencies exceeding ca. 300,000 plates per meter, with permeability comparable to that of columns packed with 3 μm particles [5,8]. Thus, columns packed with superficially porous particles offer efficiencies comparable to those achieved with the best columns packed with sub-2 μm particles, but can be operated with the same instruments as those used for conventional columns. The reduced height equivalent to a theoretical plate of columns packed with superficially porous particles for low molecular weight compounds was found [5,8] to be much smaller (1.15–1.4) than that of packed with totally porous ones (2.1–2.2).

The mass transfer mechanism in Halo-C18 packed columns (Advanced Material Technology, Wilmington, DE, USA) was investigated from a theoretical [7,9,10] and an experimental point of view [5,11]. The reduced B term of the van Deemter equation is smaller for columns packed with superficially porous particles than for those packed with fully porous particles (~25%). This result is explained by the smaller internal porosity of the particles, which provides a smaller volume accessible for sample diffusion [5]. The reduced C-term for small molecular weight compounds is practically the same for both types of particles because the effective intra-particle diffusivity of low molecular weight compounds is so large that the intra-particle mass transfer resistance is negligible in both cases [12]. The reduced A term is lower for columns packed with superficially than with fully porous particles. This may

* Corresponding author at: University of Tennessee, Department of Chemistry, 552 Buehler Hall, Knoxville, TN, 37996-1600, USA. Tel.: +1 8659740733; fax: +1 8659742667.
E-mail address: guiochon@ion.chem.utk.edu (G. Guiochon).

0021-9673/$ – see front matter © 2010 Elsevier B.V. All rights reserved.
doi:10.1016/j.chroma.2010.08.013

in part be due to the narrow particle size distribution of superficially porous particles, and probably in part to the high friction coefficient between superficially porous particles that have rough surfaces, which decreases the amount of strain taking place during consolidation of the packed bed. Electrochemical measurements of the local flow velocity across the column [11] demonstrated, however, similar amplitude of the flow velocity gradient across columns packed with either totally or superficially porous particles.

Using the four basic models of mass transfer kinetics in chromatographic columns, the general rate model, the POR, the transport-dispersive, and the equilibrium-dispersive models, Kaczmarski and Guiochon [10] modeled the efficiency of columns packed with superficially porous particles. These authors calculated the HETP curves for molecules having different molecular masses and sizes. Their results showed that, for compounds having a large molecular size, such as proteins, the column efficiency increases with decreasing thickness of the porous shell, due to the decrease of the rate of mass transfer with increasing molecular size and with increasing shell thickness. In contrast, for small-size molecules, the change of column efficiency with shell thickness is negligible. However, the authors investigated the mass transfer kinetics of superficially porous particles as a function of the mere shell thickness but they did not discuss whether there is an optimum shell thickness or ratio of the thickness of the porous layer to the diameter of the solid core, optimum that would maximize the resolution of some pairs of compounds.

The aim of this work was to investigate the effect of the shell thickness on the resolution between different types of molecules and to evaluate the influence of this thickness on isocratic and gradient Poppe plots. The importance of the extra-column contribution to band broadening on the efficiency of this separation will also be discussed.

2. Theory

The resolution, R_s, of two compounds is a numerical measure of the degree of their separation. R_s can be calculated from the statistical moments of the chromatographic peaks as

$$R_s = \frac{1}{2}\frac{|\mu_{1a} - \mu_{1b}|}{\sqrt{\mu_{2a}} + \sqrt{\mu_{2b}}} \tag{1}$$

where $\mu_{1a/b}$ is the first moment (retention time or volume) of the peaks of compounds a or b, and $\mu_{2a/b}$ is their variances.

The general rate model permits the calculation of the statistical moments of a peak eluted from a column using either fully or superficially porous stationary phases as a function of the characteristics of the phase system, the components involved, and the thickness of the particle shell [10]:

$$\mu_{1,\mathrm{col}} = \frac{L}{u}\left[1 + \frac{(1-\varepsilon_e)(1-\rho^3)}{\varepsilon_e}(K_a(1-\varepsilon_p) + \varepsilon_p)\right] \tag{2}$$

$$\mu_{2,\mathrm{col}} = \frac{2L}{u}(\delta_{ax} + \delta_f + \delta_d) \tag{3}$$

where L is the column length, u the interstitial velocity of the mobile phase, ε_e the external bed porosity, ε_p the porosity of the porous shell, K_a the adsorption equilibrium constant (Henry constant), and δ_{ax}, δ_f, and δ_d are the contributions of axial dispersion, film mass transfer, and pore diffusion processes to the apparent band dispersion, which can be expressed as [10]

$$\delta_{ax} = \frac{D_L}{u^2}\left[1 + \frac{(1-\varepsilon_e)(1-\rho^3)}{\varepsilon_e}(K_a(1-\varepsilon_p) + \varepsilon_p)\right]^2 \tag{4}$$

$$\delta_f = \frac{r_p}{3k_f}\frac{(1-\varepsilon_e)(1-\rho^3)^2}{\varepsilon_e}\left[K_a(1-\varepsilon_p) + \varepsilon_p\right]^2 \tag{5}$$

Table 1
Parameters.

		Small molecule	Medium peptide	Large peptide	Protein
D_m	$\frac{cm^2}{min}$	6×10^{-4}	1.2×10^{-4}	6×10^{-5}	2.5×10^{-5}
γ_p		0.55	0.45	0.35	0.31
γ_e		0.6	0.6	0.6	0.6
ε_p		0.4	0.28	0.13	0.05
ε_e		0.4	0.4	0.4	0.4
ξ		0.08	0.21	0.32	0.68
ω_1			1/100	1/100	1/100
λ_1			1/6	1/6	1/6
ω_2			1/5	1/5	1/5
λ_2			1/5	1/5	1/5
ω_3			See Eq. (15)	See Eq. (15)	See Eq. (15)
λ_3			0.576	0.576	0.576

$$\delta_d = \frac{\beta r_p^2}{15 D_{\mathrm{shell}}}\frac{1-\varepsilon_e}{\varepsilon_e}\left[K_a(1-\varepsilon_p) + \varepsilon_p\right]^2 \tag{6}$$

where D_L is the axial dispersion coefficient, k_f the external mass transfer coefficient, D_{shell} the pore diffusion coefficient of the solute in the shell of the particles, and β is given by the relationship

$$\beta = (1-\rho^3)^2\frac{1 + 2\rho + 3\rho^2 - \rho^3 - 5\rho^4}{(1 + \rho + \rho^2)^2} \tag{7}$$

In Eqs. (2)–(7) ρ represents the ratio of the radius of the inner solid core, r_{core}, to the radius of the particle, r_p:

$$\rho = \frac{r_{\mathrm{core}}}{r_p} \tag{8}$$

Accordingly, ρ is zero for fully porous particle and one for non-porous particles.

The retention factor, k, of a compound can be calculated from Eq. (2), considering that the hold-up time of the column, t_0, is equal to the first statistical moment of the band of a non-retained compound ($K_a = 0$). Accordingly,

$$k = K_a\frac{(1-\varepsilon_e)(1-\rho^3)(1-\varepsilon_p)}{\varepsilon_e + (1-\varepsilon_e)(1-\rho^3)\varepsilon_p} \tag{9}$$

The fraction on the right hand side of Eq. (9) is the phase ratio or ratio of the volume of porous stationary phase to the volume occupied by the mobile phase in the column. Note that Eq. (3) does not include the contribution of a finite rate of adsorption. As most authors of theoretical work in chromatography, we consider the rate of adsorption to be infinite and ignore it in the calculations.

3. Experimental

The separation power of superficially porous particles was investigated for four molecules of different sizes: small molecules (molecular weight, M, <500), medium-sized peptides ($M \simeq 1000$), large peptides ($M \simeq 6000$), proteins ($M \simeq 60{,}000$). The values of the numerical parameters necessary for the numerical calculations, such as the internal and external column porosities, the Henry constants, the ratios of the molecule size and the average pore diameter, the molecular diffusivities, the parameters of "eddy" diffusion terms of the HETP equation, and the obstruction factors are listed in Table 1. Note that, due to the exclusion of the larger molecules from the smaller pores, the porosity of the porous layer (ε_p) differs significantly from sample to sample, depending on their molecular size. This effect is used for the determination of ε_p, and ε_e by inverse size exclusion chromatography (see e.g. Figs. 5–7 of Ref. [13] for superficially, and Fig. 1 of Ref. [14] for fully porous particles). In all the calculations, the column length and diameter were assumed to be 10 cm and 2.1 mm, respectively, while the particle diameters were set to 2.6 μm. The average pore size of the porous layer was assumed to be 100 Å. It was also assumed that the

shape and size distribution of the particles are the same, regardless of the shell thickness and that the quality of the column packing remains identical in all cases. The calculations were carried out by Mathematica 7.0 ran under the GNU Linux operating system (blackPanther OS).

4. Results and discussion

4.1. HETP curves for totally and superficially porous particles

The height equivalent to a theoretical plate, HETP, can be calculated from the statistical moments of the peak eluted [see Eqs. (2) and (3)] as

$$H = L\frac{\mu_{2,\mathrm{col}}}{\mu_{1,\mathrm{col}}^2} \tag{10}$$

Further calculations require knowledge of some kinetic and structural parameters like the axial dispersion coefficient, D_L, the external mass transfer coefficient, k_f, and the diffusion coefficient of the compound in the porous shells of the particles, D_{shell}.

The axial dispersion coefficient can be approximated as the sum of the longitudinal molecular diffusion and the "eddy" diffusion:

$$D_L = \left[\gamma_e + \frac{1-\varepsilon_e}{\varepsilon_e}(1-\rho^3)\Omega\right] D_m + h_{\mathrm{eddy}} r_p u \tag{11}$$

where

$$\Omega = \varepsilon_p \gamma_p \left[(1-\xi)^2(1-2.104\xi+2.09\xi^3-0.956\xi^5) + \frac{\alpha K_a}{1+0.5K_a}\right] \tag{12}$$

γ_e and γ_p are the obstruction factors of the packed bed and the mesopores in the particle, respectively, ξ is the ratio of the molecule and the average pore diameter, α is a factor describing the structure of the surface of the stationary phase ($\alpha \simeq 3$), and h_{eddy} is the contribution of "eddy" diffusion to the reduced height equivalent to a theoretical plate. h_{eddy} can be approximated as the sum of the trans-channel, short-range interchannel, and trans-column eddy diffusion terms [15]:

$$h_{\mathrm{eddy}} = \sum_{i=1}^{3} \frac{1}{(1/2\lambda_i) + (1/\omega_i \nu)} \tag{13}$$

where λ_is and ω_is are parameters representing the flow and diffusion exchange mechanisms at different ranges ($i=1$ trans-channel, $i=2$ short-range interchannel, $i=3$ trans-column effect), and ν is the reduced interstitial velocity

$$\nu = \frac{u 2 r_p}{D_m} \tag{14}$$

The first product on the right hand side of Eq. (12) containing ξ represents the hindrance diffusion factor [16] while the fraction represents the contribution of surface diffusion of the retained solute [17].

The ω_3 parameter of the trans-column eddy diffusion term was calculated by the following expression:

$$\omega_3 = \frac{2.4\times 10^{-8} d_c^2 \varepsilon_e}{4 r_p^2 \left[\gamma_e \varepsilon_e + (1-\rho^3)(1-\varepsilon_e)\beta\right]} \tag{15}$$

The external mass transfer coefficients can be calculated using the Wilson–Genkoplis correlation [18]. The validity of this equation in chromatography was confirmed for fully porous [19] and for non-porous particles [20]

$$k_f = \frac{1.09}{\varepsilon_e}\frac{D_m}{2r_p}(\varepsilon_e \nu)^{1/3} \tag{16}$$

The sample diffusivity in the porous layer, D_{shell}, is expressed as

$$D_{\mathrm{shell}} = D_m \Omega \tag{17}$$

The values of the constants necessary for the calculation of Eqs. (11)–(17) are collected in Table 1 for a typical small molecule (e.g. caffeine, or phenol), a medium-sized peptide (e.g. bradykinin, or kallidin), a large peptide (e.g. insulin), and a medium-sized protein (e.g. bovine serum albumin, BSA). All the parameters of Table 1 were chosen to represent a typical chromatographic stationary phase particle regardless of its superficially or fully porous structure. The only exceptions were the values of λs and ωs necessary for the calculation of the "eddy" term, which are obtained from experimental results of Gritti et al. [13] determined for a Kinetex column (2.6 μm, Phenomenex, Torrance, CA, USA).

Fig. 1a–d shows the reduced HETP, h, curves calculated for the four different molecules, for fully and for superficially porous particles, with K_a set to be 3.0. The retention factors, k, of the different compounds calculated by Eq. (9) for fully porous particles ($\rho = 0$) were 1.69, 2.28, 3.28, and 3.98 for small molecules, medium-sized peptides, large peptides, and medium-sized proteins, respectively. The extra-column band broadening contributions to the peak widths was neglected in the calculations of these curves. The amount of sample injected was small, corresponding to the linear range of the isotherm and kept proportional to the shell volume. The values of the resolutions discussed in the following sections are based on Fig. 1a–d.

A comparison of the curves in these figures shows the effect of the shell thickness. First, the slopes of the HETP curves at high-reduced velocities are higher for the totally porous particles, their slopes decrease markedly with decreasing molecular size. The minimum values calculated for hs are smaller for superficially porous particles than for totally porous ones. For $\rho = 0.7$, these values are 1.39 (small molecule), 1.34 (medium peptide), 1.38 (large peptide), and 1.63 (protein). These values agree well with those measured and previously reported for a column packed with the Kinetex superficially porous particles (Phenomenex, Torrance, CA) [8]. In contrast, these values for totally porous particles are 1.70 (small molecule), 1.64 (medium peptide), 1.73 (large peptide), and 2.18 (protein). The minimum value of h for the protein increases markedly ($\Delta h > 0.55$, or more than 30%) when ρ decreases change from 0.7 to 0. This relative difference decreases with decreasing size of the molecule. Fig. 1d shows clearly that a 100 Å pore size is too small for the proteins chosen for the calculations (molecular diameter, $\varnothing \simeq 68$ Å) resulting in highly inefficient conditions for the separation of molecules having similar characteristics.

Finally, the minimum values of h calculated for the totally porous particles ($h \simeq 1.7$) and for small molecules and peptides that are reported in Fig. 1a–d are much smaller than those usually measured for columns packed with these particles ($h \simeq 2$). This observation demonstrates that the improvement in column efficiency that is observed with superficially porous particles cannot be explained only by their unique structure. There are two possible explanations for this result. The manufacturing of superficially and fully porous particles uses different processes, leading to different characteristics. First, the particle size distributions of superficially porous particles are much narrower than that of fully porous particles. The $d90/10$ size ratio of the former is around 1.13, and that of the latter is between 1.5 and 2.0 [8]. This narrow size distribution of superficially porous particles may have a significant effect on the "eddy" diffusion term of the reduced plate height, explaining the better efficiency [4,6] (note that the λ and ω parameters of the "eddy" term were obtained from experimental data on superficially porous particles [13]). Alternately, the surface of the particles of fully porous particles is much smoother than that of superficially porous particles [8]. Thus, the friction coefficients between particles and between bed and column wall are lower for the former,

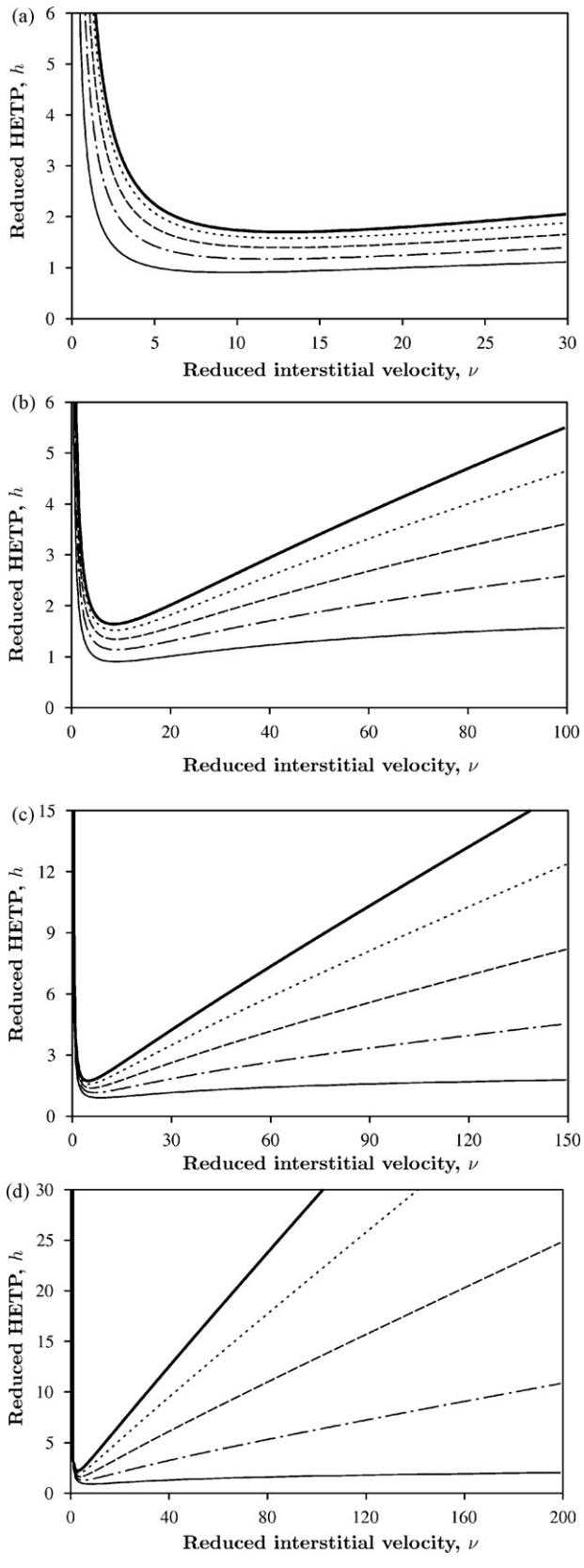

Fig. 1. Reduced plate heights of compounds having different molecular sizes as a function of the reduced velocity, for different thickness of the porous layer—$\rho = 1$: solid line; $\rho = 0.85$: dot-dashed line; $\rho = 0.7$: dashed line; $\rho = 0.5$: dotted line; $\rho = 0$: thick solid line. The Henry constants, K_a, of the compound used for the calculation is 3. (a) Small molecules; (b) medium-size peptides; (c) large peptides; (d) proteins.

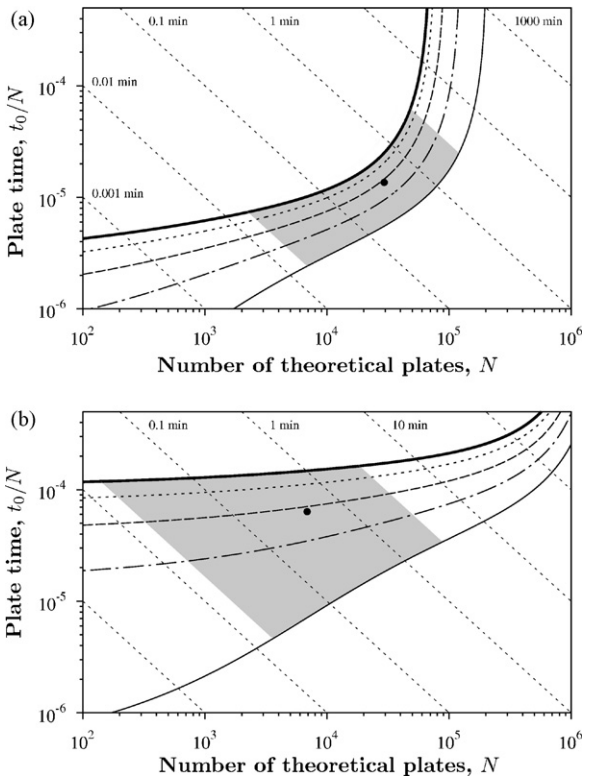

Fig. 2. Isocratic Poppe plot for (a) small molecules and (b) large peptides, for different shell thickness—$\rho = 0$: thin solid line; $\rho = 0.5$: dotted line; $\rho = 0.7$: dashed line; $\rho = 0.85$: dot-dashed line; $\rho = 0.976$: thick solid line. In both figures, the grey area represents the range of conditions used for practical separations and the black circle a calculated point for a column filled with superficially porous particles commercially available ($L = 10$ cm, 2.6 μm particles, $\rho = 0.7$). The Henry constants, K_a, of the compound used for the calculation is 3.

fully porous particles, easing stress relaxation throughout their bed during its packing but causing the formation of a significant strain distribution, hence radial porosity and permeability distributions, increasing the velocity biases across the bed and resulting in a column efficiency that is lesser for fully porous than for superficially porous particles.

4.2. Isocratic and gradient Poppe plot of superficially porous particles

Traditionally, HETP curves are used to compare the kinetic parameters of different columns and/or packing materials. However, these curves do not consider the permeability of the columns and ignore part of the information that is necessary for the optimization of separations for minimum analysis time or for maximum resolution. Poppe introduced a graphical plot [21] that visualizes the compromise between efficiency and speed of isocratic separations. In "Poppe plots", the hold-up time per theoretical plate (t_0/N) is plotted against the plate count (N) in logarithmic scale. Later, Wang et al. extended the isocratic "Poppe plot" to gradient elution [22] wherein the hold-up time, t_0, and the number of theoretical plates, N, are replaced by the gradient time, t_g, and the peak capacity, n. In Fig. 2, the isocratic "Poppe plots" of superficially porous particles are shown for small molecules (Fig. 2a) and large peptides (Fig. 2b), at different shell thicknesses. During the calculation of Fig. 2, the maximum pressure allowed for the separations was set to 400 bar in order to represent a conventional HPLC system. The column permeability factor and the eluent viscosity were assumed to be 700 and 0.001 Pa s, respectively, the column diameter was set to 0.21 cm, and the HETP curves of small molecules and large

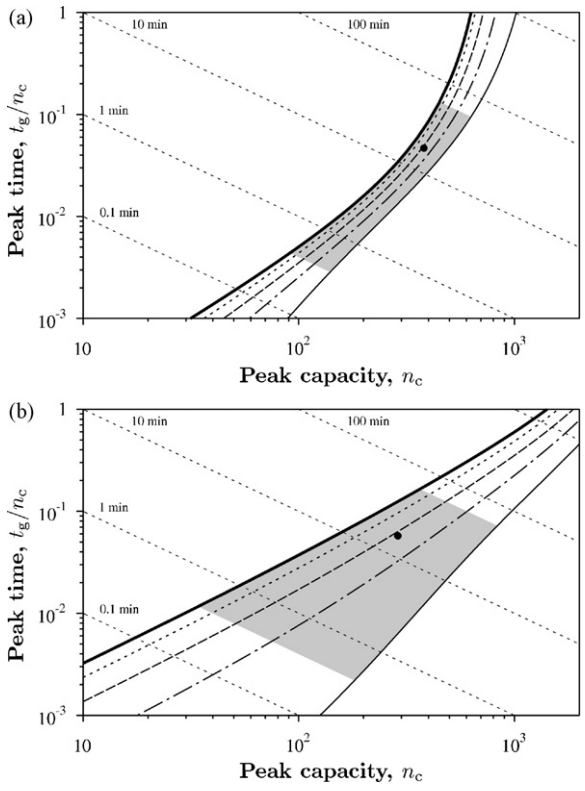

Fig. 3. Gradient Poppe plot for (a) small molecules and (b) large peptides, for different shell thickness—$\rho = 0$: thin solid line; $\rho = 0.5$: dotted line; $\rho = 0.7$: dashed line; $\rho = 0.85$: dot-dashed line; $\rho = 0.976$: thick solid line. In both figures, the grey area represents the range of conditions used for practical separations and the black circle a calculated point for a column filled with superficially porous particles commercially available ($L = 10$ cm, 2.6 μm particles, $\rho = 0.73$). The Henry constants, K_a, of the compound used for the calculation is 3.

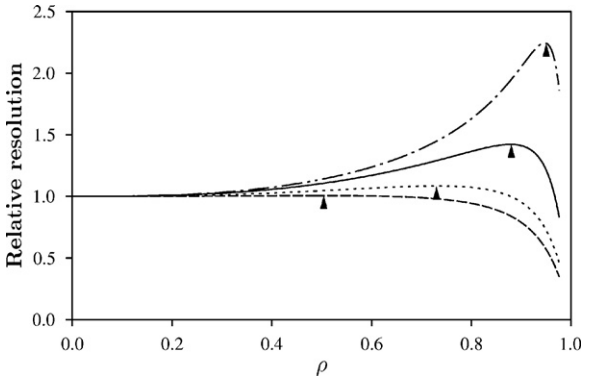

Fig. 4. Resolution of pairs of compounds having different molecular sizes. Dashed line, small molecules; dotted line, medium-size peptides; solid line, large peptides; dot-dashed line, proteins. Plots of the resolution on a column packed with superficially porous particles relative to the resolution on a column packed with fully porous particles; resolution calculated at the optimal mobile phase flow rate (0.43 ml/min). The Henry constants, K_a, of the two compounds used for the calculation are 3 and 3.5.

peptides shown in Fig. 1a–d were used. The method of calculation was the same as that in the original paper [21]. The grey areas in Fig. 2 represent the practical region of separations (t_0 between 1 s and 3 min). Fig. 2 clearly shows that the decreasing porous layer significantly affects the efficiency of the separation. The time necessary to achieve a given plate count decreases and the plate count achievable in a given time increases with decreasing porous layer thickness. Consistent with the conclusions of the previous section, Fig. 2 shows that the shell thickness has more significant effects for large molecules having a small diffusivity than for small molecules having a large diffusivity. It is important to note that, regardless of the molecular size, the efficiency increases more when ρ increases from 0.7 to 1 than when it increases from 0 to 0.7. In Fig. 3, the black circles represent data points calculated for a 2.1 × 100 mm column filled with 2.6 μm superficially porous particles with $\rho = 0.73$ (the shell thickness for the Kinetex particles).

Fig. 3 shows the gradient "Poppe plot" for superficially porous particles, small molecules and large peptides at different shell thickness. The plots were calculated according to the method described in Ref. [22]. The maximum pressure (400 bar), the column permeability factor (700), the eluent viscosity (0.001 Pa s), and the column diameter (0.21 cm) were the same as in the isocratic case. The change of concentration of the organic modifier in the eluent during the gradient run was set to 0.8, and the slope of the logarithm of the retention factor as a function of organic content of the eluent was −15 and −30 for the small molecules and the large peptides, respectively. The grey area represents the practical region of gradient times (t_g between 24 s and 60 min). Fig. 3 shows that the achievable peak capacity, n_c, in a given time increases with decreasing shell thickness. However, the effect of increasing the shell thickness is less significant for the small molecules than for large peptides. As in the isocratic case, the real advantage of a thin shell emerges only when the shell thickness becomes less than 20% of the particle radius ($\rho > 0.8$), which is less than the shell thickness of particles commercially available. The black circles represent a point calculated for a 2.1 mm i.d., 10 cm long column filled with 2.6 μm superficially porous particles ($\rho = 0.73$).

The achievable peak capacity of that column is between 280 and 380, in less than 18 min, depending on the nature of the sample components. However, this value is an overestimate because, during the calculation made to arrive at Fig. 3, it was assumed that the sample peaks elute from 0 to t_g. In practice, this is usually not true and the conditional peak capacity, n_c, which is calculated on the basis of the first and last eluting peaks, is always smaller than the peak capacity calculated on the basis of t_g. Furthermore, the extra-column processes that broaden peaks and reduce the peak capacity were neglected during the calculations. Consistent with these results, Gritti and Guiochon [23] obtained a ∼170–180 conditional peak capacity for the resolution of a β-lactoglobulin digest on superficially porous particles.

Figs. 2 and 3 illustrate how commercially available columns packed with superficially porous particles can provide a significantly higher separation power than fully porous particles, especially for molecules with low diffusivity.

The comparison of the performance of a 2.1 mm i.d. column and a conventional 4.6 mm i.d. column is unusual. Note, however, that the trends shown in Figs. 2 and 3 are independent of the column diameter provided that the sample size is adjusted accordingly.

4.3. *Effect of thickness of porous shell on the chromatographic resolution*

In the previous sections, chromatographic column packed with superficially porous particles were shown to provide higher column efficiencies, N, than columns packed with fully porous particles. However, the most important measure of a chromatographic separation power is not N but the resolution, R_s, between different compounds, which depends not only on the number of theoretical plates but also on the difference between the retention times of the compounds considered. Thus, the actual resolution between two closely eluted compounds on superficially porous particles depends on how both the peak widths and the difference between their retention times, functions of the structure of the particles. Fig. 4 shows the effect of the shell thickness on the resolution of pairs of

components of different types, as calculated by Eqs. (1)–(9), with the parameters listed in Table 1. In order more consistently to compare the resolutions between the different types of molecules, the Henry constants, K_a, of the less retained molecules of each pair was set to be 3 and that of the other compound to be 3.5, independently of the size of the molecules. This choice eliminates the effect of the adsorption equilibrium on the retention times and the peak widths. The calculated resolutions were divided by the resolution of the same pairs calculated for totally porous particles. Thus, Fig. 4 shows relative resolutions. The eluent flow rate was set at the optimum flow rate for small molecules (0.43 ml/min, see Fig. 1). The minimum thickness of the porous shell was assumed to be 30 nm, a value close to the size of the colloid silica particles that might be attached to the solid silica core.

Close examination of Fig. 4 highlights how changing the shell significantly affects the resolution of pairs of compounds having different sizes. For each pair, the curves exhibit a maximum resolution for different shell thickness, indicated by the maximum of a peak. In the case of small molecules, the maximum resolution can be observed at $\rho = 0.50$ but the gain in R_s is negligible, merely 1%. The resolution decreases significantly when ρ exceeds 0.8. The resolution of pairs of small molecular size components becomes 2% less for the shell thickness of the commercially available superficially porous particles ($\rho = 0.65$–0.75) that is currently available. Even though Fig. 1 shows that the column efficiency can be higher (i.e., smaller h values) with superficially porous particles, the loss of column capacity that is associated with the reduction in the specific surface area of the packing material causes a decrease of the retention factors of the components in a way that compensates the efficiency gain. Below a certain value of the shell thickness, the retention factor decreases so much that this retention decrease controls the resolution, resulting in a significant decrease of R_s. In conclusion, the use of superficially porous particles does not offer any significant gain in the degree of separation of low molecular weight compounds as long as K_a is kept constant. In other words, some improvement in resolution can be achieved only if the retention decrease associated with the reduction in the shell thickness is compensated by a reduction of the eluent strength. This reduction can be obtained easily by changing the concentration of the organic modifier in the mobile phase, which will affect the viscosity of the mobile phase, hence the exact Poppe plot corresponding to the separation studied and the column performance. It is difficult, however, to elaborate on the final result because the viscosity of the aqueous solutions of most organic modifiers does not vary linearly with their concentrations. The viscosity is maximum for concentrations of 50% methanol and 25% acetonitrile in water. It also varies strongly with temperature. Accordingly, a modeling of the viscosity effect in the general case is too complex and will not be discussed here.

For medium-size peptides (e.g. bradykinin, which has 9 amino acid residues), the effect of changing the thickness of the porous shell is more significant. The resolution of similar peptides would increase with decreasing shell thickness until the shell volume is 60% of the particle volume (or $\rho \simeq 0.73$). The gain in resolution at this optimum thickness is slightly less than 10%. So, for these compounds the use of superficially porous phases does offer a significant advantage in separation power. The optimal thickness of the porous shell for medium-size peptides is practically the same as the thickness of the particles that are currently available on the market. A further decrease of the porous layer thickness, however, would decrease the resolution of this type of molecules, for the same reason as mentioned above for low molecular weight compounds.

Fig. 4 shows how the use of superficially porous particles may become advantageous for the separation of large peptides. The resolution of compounds having molecular sizes around 32 Å is still satisfactory for columns packed particles having an average pore size of the order of 100 Å. The resolution increases significantly with decreasing thickness of the porous shell. At $\rho = 0.70$, the resolution gain exceeds 25%. However, the optimum shell thickness corresponds to a volume of porous silica that is ~35% of the total particle volume (i.e., $\rho = 0.87$). Then, the resolution gain is more than 40%. Fig. 4 suggests that the efficiency of commercially available superficially porous particles could be improved significantly.

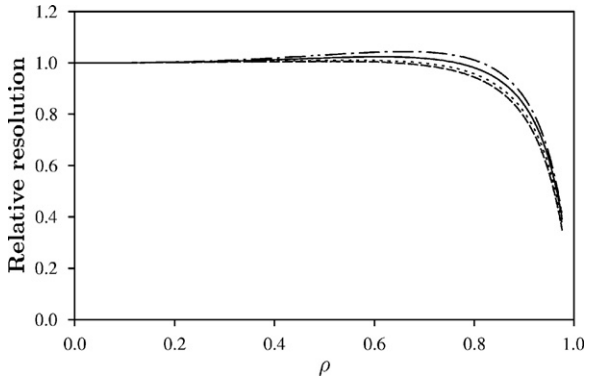

Fig. 5. Resolution of pairs of compounds having different molecular sizes. Dashed line, small molecules; dotted line, medium size peptides; solid line, large peptides; dot-dashed line, proteins. Plots of the resolution on a column packed with superficially porous particles relative to the resolution on a column packed with fully porous particles; resolution calculated at the optimum mobile phase flow rate, 0.43 ml/min for small molecules; 0.057 ml/min for medium size peptides; 0.016 ml/min for large peptides; and 0.0037 ml/min for proteins. The Henry constants, K_a, of the two compounds used for the calculation are 3 and 3.5.

In the case of large proteins, the effect of decreasing the shell thickness is remarkable. The increase of R_s is ~40% at $\rho = 0.70$, much better than the resolution gain obtained for large peptides. The possible gain in resolution is increased by 140% when the thickness of the porous shell reaches the optimum value corresponding to $\rho = 0.95$. At this thickness of the porous layer, superficially porous particles really become the superficially porous particles of Horváth and Lipsky [9]. Available for a long period, the 5 μm Poroshell 300SB particles (Agilent Technologies, Wilmington, DE, USA) have a similarly thin shell ($\rho = 0.9$). However, this phase has much wider pores (300 Å) and larger particle diameters than that was assumed during our calculations. Thus, the conclusions reached above cannot be used directly for Poroshell 300SB phase.

4.4. Optimization of the flow velocity and the shell thickness

In the previous section, column performance was calculated at the same flow rate, the optimum flow rate for small molecules ($V_F = 0.43$ ml/min). The reduced interstitial velocity, ν [see Eq. (14)], for these compounds is 13, assuming a value of $D_m = 6 \times 10^{-4}$ cm^2/min. This flow rate, however, corresponds to significantly different values of ν for compounds having larger molecular sizes and smaller molecular diffusion coefficient (see Table 1). A flow rate of 0.43 ml/min gives values of 65, 130, and 320 for the reduced interstitial flow velocity of medium-sized peptides, large peptides, and proteins, respectively. These reduced velocities are much larger than the optimum values.

Fig. 5 illustrates the effect of the shell thickness on the resolution of pairs of types of compounds having different molecular sizes. In this figure, the relative resolutions were calculated at the optimum flow rate for these different pairs of compounds, even if the use of this flow rate is impractical in certain cases (e.g. large peptides and proteins). Accordingly, the flow rates were assumed to be 0.43, 0.057, 0.016, and 0.0037 ml/min for small molecules; medium-size peptides; large size peptides; and proteins, respectively. The results shown in Fig. 5 differ fundamentally from those

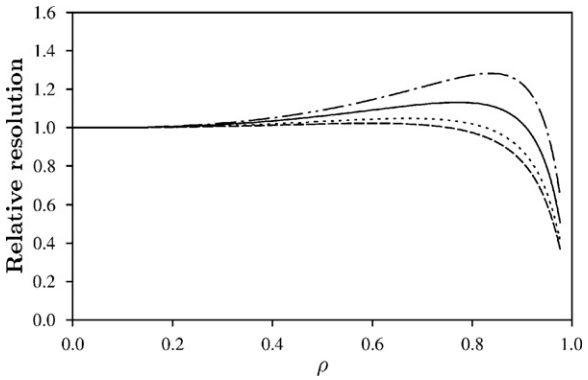

Fig. 6. Same as Fig. 5 except that the resolutions were calculated at a flow rates four times larger than the optimum flow rates for the different compounds that were used in Fig. 5.

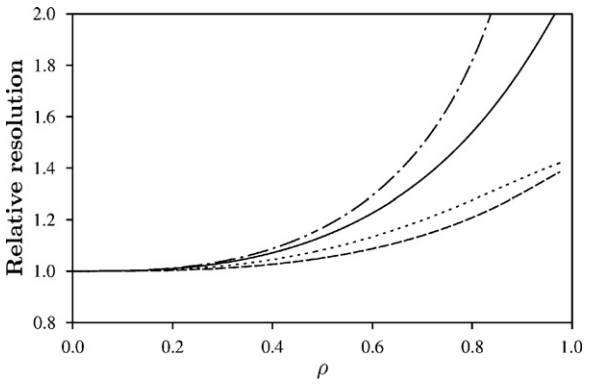

Fig. 7. Resolution of pairs of compounds having different molecular sizes (dashed line, small molecules; dotted line, medium size peptides; solid line, large peptides; dot-dashed line, proteins) after retention compensation. Plots of the resolution on a column packed with superficially porous particles relative to the resolution on a column packed with fully porous particles; resolution calculated at the optimum mobile phase flow rate, 0.43 ml/min for small molecules.

shown in Fig. 4. The influence of the shell thickness on the column performance is small at best, negligible in most cases. The largest resolution gain is less than 5% (with $\rho = 0.66$) for the proteins, slightly more than the 2% gain (with $\rho = 0.61$) for the large peptides, and the 1% gain (with $\rho = 0.55$) for the medium-size peptides. The optimum shell thicknesses decrease significantly with increasing molecular size but this increase is much less important than under the experimental conditions of Fig. 4.

Fig. 6 shows what may happen when separations are carried out at too large a flow rate, e.g. to save time. The same curves as in Figs. 4 and 5 were calculated but at flow rates four times larger than the optimum ones. Under such conditions, the actual resolutions between the pairs of compounds decrease since the HETP increases. As the flow rate is increased, however, the relative gain in resolution also increases, consistent with the slope of the HETP curves at high flow rates (see Fig. 1a–d). As expected, the maximal gain of resolution does not change much ($\Delta R_s \simeq 2\%$, with $\rho \simeq 0.60$) for small molecules since their C coefficient is small. In the case of the medium-size peptides, the resolution gain is more than 5% (with $\rho = 0.67$), which could be considered as worthwhile since it is five times larger than the increase achieved at the optimum flow rate of this type of compounds. For the other two types of molecules, the large peptides and large proteins, the R_s increase is 13% ($\rho = 0.77$) and 28% ($\rho = 0.83$) respectively, sixfold larger than at the optimum flow rate.

The comparison of Figs. 4–6 demonstrates that even superficially porous particles do not offer a remarkable gain of resolution for pairs of compounds that are separated at the optimum flow rate for maximum efficiency. Important increases in separation power is observed only if separations are done at flow rates significantly higher than the optimum, which is always the case for large molecules. Then, their use may provide considerably increased resolutions compared to those achieved with fully porous particles. It is striking that the superficially porous particles that are commercially available (Halo, Kinetex, and Poroshell) have shell thicknesses that are close to the optimum for the separations of compounds having the molecular sizes of medium-size peptides. Larger peptides and proteins could possibly benefit from the use of thinner porous layers.

4.5. Chromatographic resolution after retention compensation

In the previous section, the Henry constants, K_a, of the different compounds were kept constant, at 3 and 3.5. Then, decreasing the shell thickness causes a decrease of the surface area of the stationary phase, resulting in a decrease of retention and eventually of the actual resolution between the two compounds, when the porous layer becomes too thin. However, in practice, analysts compensate the retention decrease by using a weaker eluent which increases the value of K_a. In Fig. 7, the resolution of pairs of compounds having different molecular sizes was calculated by fixing the retention factor ($k = (t_R - t_0)/t_0$) of the first eluting compound and by setting the K_a of the second compound to keep constant their selectivity ($\alpha = 3.5/3 = 1.17$). Fig. 7 shows that when the retention factors are kept constant, the resolutions increase with increasing value of ρ in the whole range, regardless of the size and molecular diffusivity of the compounds. This result is not surprising, considering that decreasing the thickness of the porous shell decreases the width of peaks which still have the same retention factor. As a result, the resolutions of all pairs of compounds increase. Just as was shown in the previous sections, the gain in resolution increases with decreasing molecular diffusivity.

According to Fig. 7, if the retention factor is kept constant, as assumed in this section, a significant gain in resolution could be achieved with the commercially available superficially porous particles compared to the resolution provided by fully porous particles, provided that all the other parameters of the column (length and diameter, homogeneity of the bed) and the stationary phase (surface chemistry, specific surface area, and particle size distribution) are the same. The comparison of Figs. 4 and 7 suggests that the separations between low molecular size molecules increases significantly when the eluent becomes weaker, while, in case of large molecular size compounds, the separation with retention compensation does not significantly improve. Due to the large effect of a change in the mobile phase concentration of the organic modifier on the retention of large peptides or proteins, such changes will probably affect largely the resolution of many separations. This effect, however, is specific of the particular separation performed and it is not possible to further elaborate constructively on this issue.

4.6. Effect of the extra-column volume on the achievable performance

In the calculations made to obtain the results discussed in the previous section, the effects of the extra-column volumes, V_{ext}, on the first and second moment of the eluted peak were neglected. Yet, it is not possible to operate a column without an instrument and to have an instrument with no extra-column volumes. Considering these effects, μ_1 and μ_2 should be rewritten as:

$$\mu_1 = \mu_{1,col} + \frac{V_{ext}}{F} \quad (18)$$

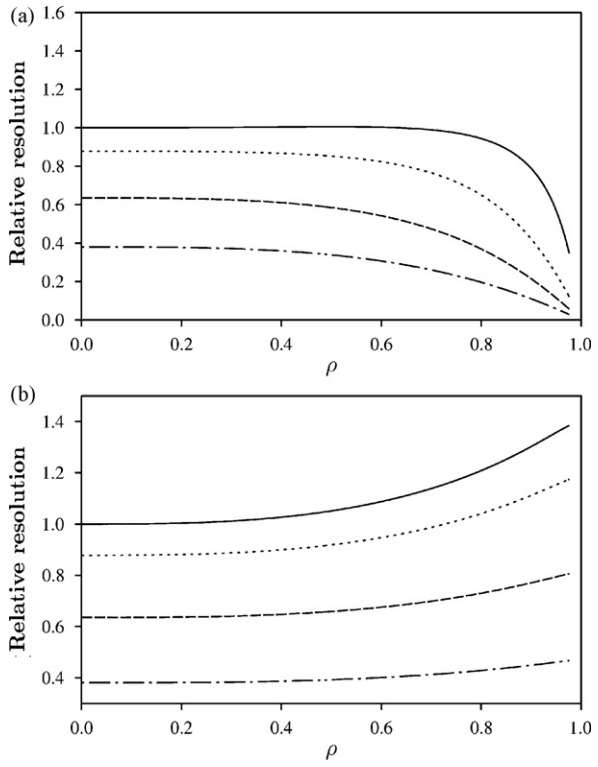

Fig. 8. Resolution of pairs of small molecular size compounds on columns packed with superficially porous particles relative to their resolutions on a column packed with fully porous particles when the contribution of extra-column processes to band broadening is significant. Resolutions calculated at the optimum flow rate for these small molecules (0.26 ml/min). The extra-column volumes were: solid line, 0 μL^2; dotted line, 5 μL^2; dashed line, 25 μL^2; and dash-dotted line, 100 μL^2. The Henry coefficients of the compound were 3 and 3.5 in (a); they were set to keep constant the retention factors of the compounds in (b).

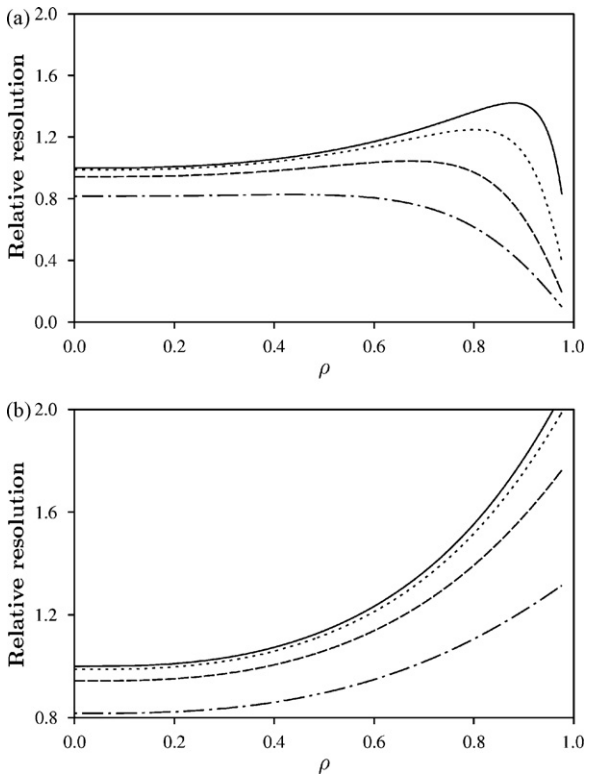

Fig. 9. Same as Fig. 8, except that the calculations were made for pair a of large peptides.

$$\mu_2 = \mu_{2,\mathrm{col}} + \mu_{2,\mathrm{ext}} \tag{19}$$

where F is the flow rate of the eluent. According to these two equations, the resolution of two compounds becomes:

$$R_{s,\mathrm{ext}} = \frac{1}{2}\frac{|\mu_{1a} - \mu_{1b}|}{\sqrt{\mu_{2a} + \mu_{2,\mathrm{ext}}} + \sqrt{\mu_{2b} + \mu_{2,\mathrm{ext}}}} \tag{20}$$

If the width of two closely eluted peaks is assumed to be the same ($\sqrt{\mu_{2a}} = \sqrt{\mu_{2b}}$), their resolution is given by

$$R_{s,\mathrm{ext}} = R_s\sqrt{\frac{\mu_{2a}}{\mu_{2a} + \mu_{2,\mathrm{ext}}}} \tag{21}$$

This equation shows that the larger the contribution of the extra-column volume to the peak moments, the lower the resolution of the pair of compounds. Furthermore, this equation shows also that the relative loss of resolution caused by the extra-column contribution to band broadening increases with increasing column efficiency because the column contribution to the peak variance decreases with increasing efficiency. Thus, the performance of a highly efficient column is more sensitive than that of a poorly efficient one to the nefarious effects of the extra-column volumes of the instrument.

Figs. 8 and 9 illustrate the effects of the extra-column volume on the resolution obtained with different shell thickness with and without retention compensation, respectively. The data shown on these figures compare the resolutions provided by columns packed with superficially porous particles of different thickness to that of columns packed with fully porous particles and those achieved with a hypothetical zero extra-column volume instrument. The numerical parameters for the extra-column contributions to the peak variance were chosen to represent $\mu_{2,\mathrm{ext}}$ values measured with VHPLC, optimized HPLC, and non-optimized HPLC systems [24], assuming that the sample volume injected is small (1–5 μL^2). Accordingly, $\mu_{2,\mathrm{ext}}$s were set to be 5, 25, and 100 μL^2, respectively.

Figs. 8 and 9 show that the resolutions decrease rapidly with increasing extra-column contribution in the case of low molecular weight compounds. For fully porous particles, the resolution of these compounds decreases by 13%, 36%, and 62% when the extra-column variance increases from zero to 5, 25, and 100 μL^2, respectively. Importantly, the loss in resolution compared to the ideal case ($\mu L^2 = 0$) increases with increasing shell thickness. This agrees well with the conclusion reached in the discussion of Eq. (21), since the variance of eluted peaks (μ_2) decreases with decreasing shell thickness. Thus, the separation of low molecular size solutes is sensitive to the band broadening contribution of the instrument. Analyst should minimize the extra-column volume of their systems more carefully than they are used to do with fully porous particles.

There are several ways to decrease the extra-column volume of chromatographic instruments [24], such as replacing the needle seat, the connectors, and the detector cell of a standard instrument for others of smaller volumes. A proper injection strategy [24] may be helpful. Because the variances of peaks eluted from larger diameter columns are also larger, the effect of the extra-column volumes is less significant for 4.6 than for 2.1 mm i.d. columns. The resolutions of larger molecular size compounds (Fig. 9), are less significantly affected than those of smaller ones. The effect of $\mu_{2,\mathrm{ext}}$ is negligible when separations are made with fully porous particles on a typical VHPLC system but, even in this case, the resolutions decrease significantly at higher $\mu_{2,\mathrm{ext}}$ values. Note, that, when the Henry constants are kept constant ($K_a = 3$ and 3.5), the resolutions are maximum for a shell thickness close to 0.75 with a 25 μL^2 extra-column variance.

5. Conclusions

Our results show that the unique structure of superficially porous particles provides significant advantages for the separation of different types of compounds, provided that the analysis be carried out carefully, knowing the consequences of the different options. Resolution analysis shows that the separation power of superficially porous particles increases with decreasing shell thickness if the strength of the eluent is decreased to compensate for the retention change caused by the decreased surface area of the stationary phase. On the other hand, if the eluent remains the same, the resolution of low molecular size compounds may decrease. The isocratic and gradient Poppe plots showed that the separation power of superficially porous particles increases significantly with decreasing thickness of the porous layer. The smaller the diffusivity of the solutes, the larger the increase of the separation power compared to that of fully porous particles.

Thus, the separation power of columns packed with these particles could be further increased by decreasing the shell thickness. However, even though a superficial reading if this work may suggest that the thickness of the porous layer should be decreased drastically (down to $\rho \simeq 0.9$–0.95) in order to increase the separation efficiency of the columns for large molecular size compounds, this is not the proper option because decreasing the shell thickness and selecting particles with large ρ values decreases markedly the loadability of the column, making column overload easier, broadening the bands and decreasing the separation efficiency.

This work shows also that, although columns packed with superficially porous particles can be used with conventional HPLC systems, the width of the bands eluting from them is narrower than that of peaks eluted from columns packed with fully porous particles. As a consequence, the extra-column volume of the chromatograph used must be significantly minimized to avoid loosing the separation power provided by these new, unique and efficient packing materials.

Glossary of symbols

δ_{ax}	contribution of the axial dispersion to the apparent band dispersion
δ_f	contribution of the film mass transfer to the apparent band dispersion
δ_d	contribution of the pore diffusion to the apparent band dispersion
D_L	axial dispersion coefficient
D_{shell}	pore diffusion coefficient
ε_e	external bed porosity
ε_p	porosity of the porous layer
F	eluent flow rate
γ_e	obstruction factor of the packed bed
γ_p	obstruction factor of the mesopores in the particle
H	height equivalent to a theoretical plate
h_{eddy}	contribution of "eddy" diffusion to the reduced H
k	retention factor of a compound
K_a	adsorption equilibrium constant (Henry constant)
k_f	external mass transfer coefficient
L	column length (cm)
λ	parameter that represents the flow exchange mechanism
$\mu_{1/2}$	first or second statistical moment of the peak of compound eluted
N	number of theoretical plates
n	peak capacity
n_c	conditional peak capacity
ν	reduced interstitial velocity
ω	parameter that represents the diffusion exchange mechanism
r	ratio of the number of collected fractions and the peak capacity
ρ	ratio of the radius of the inner solid core, r_c, to the radius of the particle, r_p
r_c	radius of the inner solid core
r_p	radius of the particle
R_s	chromatographic resolution
t_0	hold-up time of the column
t_g	gradient time
u	interstitial velocity of the eluent
V_{ext}	extra-column volume
ξ	ratio of the molecule and the average pore diameter

Acknowledgments

This work was supported in part by Grant DE-FG05-88-ER-13869 of the US Department of Energy and by the cooperative agreement between the University of Tennessee and Oak Ridge National Laboratory.

References

[1] K. Nakanishi, N. Soga, J. Am. Ceram. Soc. 74 (1991) 2518.
[2] H. Minakuchi, K. Nakanishi, N. Soga, N. Ishizuka, N. Tanaka, Anal. Chem. 68 (1996) 3498.
[3] K. Cabrera, G. Wieland, D. Lubda, K. Nakanishi, N. Soga, H. Minakuchi, K. Unger, Trends Anal. Chem. 17 (1998) 50.
[4] J. Kirkland, Anal. Chem. 41 (1969) 218.
[5] F. Gritti, A. Cavazzini, N. Marchetti, G. Guiochon, J. Chromatogr. A 1157 (2007) 289.
[6] J.J. DeStefano, T.J. Langlois, J.J. Kirkland, J. Chromatogr. Sci. 46 (2008) 254.
[7] A. Cavazzini, F. Gritti, K. Kaczmarski, N. Marchetti, G. Guiochon, Anal. Chem. 79 (2007) 5972.
[8] F. Gritti, I. Leonardis, D. Shock, P. Stevenson, A. Shalliker, G. Guiochon, J. Chromatogr. A 1217 (2010) 1589.
[9] Cs. Horváth, S.R. Lipsky, J. Chromatogr. Sci. 7 (1969) 109.
[10] K. Kaczmarski, G. Guiochon, Anal. Chem. 79 (2007) 4648.
[11] K.S.M. Jude, A. Abia, G. Guiochon, J. Chromatogr. A 1216 (2009) 3185.
[12] F. Gritti, G. Guiochon, J. Chromatogr. A 1216 (2009) 4752.
[13] F. Gritti, I. Leonardis, J. Abia, G. Guiochon, J. Chromatogr. A 1217 (2010) 3819.
[14] S. Bocian, P. Vajda, A. Felinger, B. Buszewski, Anal. Chem. 81 (2009) 6334.
[15] J.C. Giddings, Dynamics of Chromatography, Marcel Dekker Inc., New York, 1965.
[16] E. Renkin, J. Gen. Physiol. 38 (1954) 225.
[17] K. Miyabe, G. Guiochon, J. Chromatogr. A 961 (2002) 23.
[18] E.J. Wilson, C.J. Geankoplis, Ind. Eng. Chem. Fundam. 5 (1966) 9.
[19] K. Miyabe, Y. Kawaguchi, G. Guiochon, J. Chromatogr. A 1217 (2010) 3053.
[20] K. Miyabe, M. Ando, N. Ando, G. Guiochon, J. Chromatogr. A 1210 (2008) 60.
[21] H. Poppe, J. Chromatogr. A 778 (1997) 3.
[22] X. Wang, D.R. Stoll, P.W. Carr, P.J. Schoenmakers, J. Chromatogr. A 1125 (2006) 177.
[23] F. Gritti, G. Guiochon, J. Chromatogr. A 1217 (2010) 1604.
[24] F. Gritti, C.A. Sanchez, T. Farkas, G. Guiochon, J. Chromatogr. A 1217 (2010) 3000.